ISSN 1069-3513, Izvestiya, Physics of the Solid Earth, 2013, Vol. 49, No. 6, pp. 844–858. © Pleiades Publishing, Ltd., 2013.
Original Russian Text © A.A. Zhamaletdinov, M.S. Petrischev, A.N. Shevtsov, V.V. Kolobov, V.N. Selivanov, M.B. Barannik, E.D. Tereshchenko, V.F. Grigoriev, P.A. Sergushin, E.A. Kopytenko, M.A. Birulya, A.A. Skorokhodov, O.A. Esipko, R.V. Damaskin, 2013, published in Fizika Zemli, 2013, No. 6, pp. 99–115.

Electromagnetic Sounding of the Earth's Crust in the Region of Superdeep Boreholes of Yamal-Nenets Autonomous District using the Fields of Natural and Controlled Sources

A. A. Zhamaletdinov[a, b, c], M. S. Petrischev[a], A. N. Shevtsov[b], V. V. Kolobov[c], V. N. Selivanov[c], M. B. Barannik[c], E. D. Tereshchenko[d], V. F. Grigoriev[d], P. A. Sergushin[a], E. A. Kopytenko[a, e], M. A. Birulya[e], A. A. Skorokhodov[a], O. A. Esipko[f], and R. V. Damaskin[g]

[a] *St. Petersburg Branch, Pushkov Institute of the Terrestrial Magnetism, Ionosphere and Radio Wave Propagation, Russian Academy of Sciences, Muchnoi per. 2, St. Petersburg, 191023 Russia*

[b] *Geological Institute, Kola Scientific Centre, Russian Academy of Sciences, ul. Fersmana 14, Apatity, 184209 Russia*

[c] *Center for Physical and Technological Problems of Energy in Northern Areas, Kola Science Centre, Russian Academy of Sciences, ul. Fersmana 14, Apatity, Murmansk oblast, 184209 Russia*

[d] *Polar Geophysical Institute, Kola Science Centre, Russian Academy of Sciences, ul. Fersmana 14, Apatity, Murmansk oblast, 184209 Russia*

[e] *OOO VEGA, St. Petersburg, Russia*

[f] *OAO Nedra Scientific Production Center, Yaroslavl, Russia*

[g] *Yamal-Nenets Enterprise of Main Electric Networks of Western Siberia, Russia*

Received February 1, 2012; in final form, February 13, 2013

Abstract—Electromagnetic soundings with the fields of natural (magnetotelluric (MT), and audio magnetotelluric (AMT)) and high-power controlled sources have been carried out in the region of the SG-6 (Tyumen) and SG-7 (En-Yakhin) superdeep boreholes in the Yamal-Nenets autonomous district (YaNAD). In the controlled-source soundings, the electromagnetic field was generated by the VL Urengoi-Pangody 220-kV industrial power transmission line (PTL), which has a length of 114, and ultralow-frequency (ULF) Zevs radiating antenna located at a distance of 2000 km from the signal recording sites. In the soundings with the Urengoi–Pangody PTL, the Energiya-2 generator capable of supplying up to 200 kW of power and Energiya-3 portable generator with a power of 2 kW were used as the sources. These generators were designed and manufactured at the Kola Science Center of the Russian Academy of Sciences. The soundings with the Energiya-2 generator were conducted in the frequency range from 0.38 to 175 Hz. The external generator was connected to the PTL in upon the agreement with the Yamal-Nenets Enterprise of Main Electric Networks, a branch of OAO FSK ES of Western Siberia. The connection was carried out by the wire-ground scheme during the routine maintenance of PTL in the nighttime. The highest-quality signals were recorded in the region of the SG-7 (En-Yakhin) superdeep borehole, where the industrial noise is lowest. The results of the inversion of the soundings with PTL and Zevs ULF transmitter completely agree with each other and with the data of electric logging. The MT–AMT data provide additional information about the deep structure of the region in the low-frequency range (below 1Hz). It is established that the section of SG-6 and SG-7 boreholes contains conductive layers in the depth intervals from 0.15 to 0.3 km and from 1 to 1.5 km. These layers are associated with the variations in the lithological composition, porosity, and fluid saturation of the rocks. The top of the poorly conductive Permian-Triassic complex is identified at a depth of about 7 km. On the basis of the MT data in the lowest frequency band (hourly and longer periods) with the observations at the Novosibirsk observatory taken into account, the distribution of electric resistivity up to a depth of 800 km is reconstructed. This distribution can be used as additional information when calculating the temperature and rheology of the lithosphere and upper mantle in West Siberia. The results of our studies demonstrate the high potential of the complex electromagnetic soundings with natural and controlled sources in the study of deep structure of the lithosphere and tracing deep oil-and-gas-bearing horizons in the sedimentary cover of the West Siberian Platform within the Yamal-Nenets autonomous district.

DOI: 10.1134/S1069351313050133

INTRODUCTION

Alongside seismic prospecting, electric prospecting has a high potential in the search for deep mineral resources. Electric conductivity can be treated as a proxy for the material composition, temperature, and fluid conditions in the Earth's interior. This parameter can also carry indirect information about the porosity and structural pattern of deep electrically conductive channels, on the presence of the zones of partial melting, and on the rheological conditions in the lithos-

phere. The fact that electric resistivity contains information on a large number of physical parameters of the medium and can vary in very wide limits is both advantageous and disadvantageous, since these factors enhance the ambiguity of the solution of the inverse problem. The diffusive nature of the signals confined by the framework of quasi-stationary approximation significantly limits the resolution of deep electric prospecting. One of the ways to improve its reliability is to increase the accuracy of finding the response function of the medium.

In this respect, electromagnetic sounding with a high-power controlled source (controlled-source electromagnetic sounding, CSEMS) in combination with magnetotelluric sounding (MTS) is of particular interest. The main advantage of SCEMS lies in the fact that the location and configuration of the source are precisely known and it is therefore possible to select the optimal frequency interval of sounding. Modern high-power generators (Velikhov et al., 1994; Tereshchenko et al., 2008; Barannik et al., 2009) and computer-aided digital measurement systems (Ingerov, 2011; Kolobov et al., 2011; Kopytenko et al., 2010) allow geophysicists to accumulate and reliably record the signals against strong industrial noise.

However, these advantages of SCEMS are inhibited by the disadvantages of this method such as the high cost of the works associated with the need to use expensive generator equipment and electric current lines, strict requirements for the techniques of data processing and interpretation, and a series of other factors (Zhamaletdinov, 2012). Considering this, it is not surprising that deep geoelectrics is dominated by methods of magnetotelluric and audio magnetotelluric sounding (MTS-AMTS) (Berdichvsky, 1968). The soundings with high-power controlled sources present a rare exception. Nevertheless, rapid progress in computer-aided technologies and the development of new approaches in the electromagnetic sounding theory, together with the upgrades in the instrumental base allow geophysicists to successfully solve practical problems of MTS and high-power CSEMS. Therefore, parallel development in these two directions, which are compete and complement each other, is an important prerequisite of achieving success. In this paper, we describe the first experience in conducting such investigations in the Yamal-Nenets autonomous district in the region of the SG-6 and SG-7 superdeep boreholes. The study was carried out in 2011 and 2012 by the Kola Science Center of the Russian Academy of Sciences, with the participation of the St. Petersburg Institute of Terrestrial Magnetism, Ionosphere, and Radio Wave Propagation and OOO VEGA. These works were supported by the administration of the Yamal-Nenets Autonomous District (YaNAD) and Yamal-Nenets Enterprise of Main Electric Networks—a branch of OAO FSK ES of Western Siberia.

AN OUTLINE OF THE REGION OF STUDY

The region of the study is illustrated in Fig. 1a, which shows the location of the high-voltage Urengoi-Pangody power transmission line (PTL). The dashed-dotted lines 1 and 2 contour the regions available for electromagnetic sounding with Energiya-2 (with a power of up to 200 kW) or Energiya-3 (with a power of 2 kW) generators connected to the Urengoi-Pangody PTL (contours 1 and 2, respectively). The locations of the SG-6 (Tyumen) and SG-7 (En-Yakhin) superdeep boreholes and the main potentially gas-bearing regions within YaNAD are also shown in Fig. 1a. On the right (Fig. 1b), the points of the sounding with controlled and natural sources located at distances of 25 to 100 km from the Urengoi-Pangody PTL and in the field of the ULF Zevs antenna are indicated.

The SG-6 well with its bottomhole at a depth of 7502 m is drilled 60 km east of the vast Nizhnii Urengoi gas field in the region of positive potential (gravity) fields (Megerya et al., 2012). This gas field is confined to the Urengoi swell established from the electric data obtained by magnetovariational profiling in the early 1960s (Berdichevsky, 1968). The SG-6 borehole drilled through the most complete section of Early Jurassic and Permian–Triassic sediments. However, it had not reached the Paleozoic basement, which prevented geophysicists from estimating its probable gas and oil capacity. Due to technical reasons, the drilling of the SG-6 borehole was stopped in 1994 (Esipko, Gorbachev, and Sokolova, 2000).

The SG-7 borehole was drilled in 2000 within the Bol'shoi Urengi hydrocarbon field, at the Pestsovyi swell 160 km northwest of SG–6 in the zone of negative gravity fields. This borehole reached a depth of 8250 m, which is the largest depth ever reached within sedimentary basins in Russia. At a depth of 6920 m, this borehole penetrated the alkaline Cenozoic effusive rocks (basalts) of the Permian–Triassic trap formation, which are analogous to the traps of the Siberian Platform (Gorbachev et al., 2007; Khakhaev et al., 2008). The SG-6 borehole entered the trap basalts at a shallower depth of 6500 m. Figure 2 presents the results of electrical logging (marked by circle 1) and the averaged porosity curve for the core sample from the borehole (marked by circle 2). The right-hand panels in Figs. 2a and 2b present composite columns of geological sections for both boreholes.

Below, we describe the geological cross section and logging data by the example of the SG-6 borehole (Esipko, Gorbachev, and Sokolova, 2000). The description for the SG-6 borehole is also valid for SG-7 (Gorbachev et al., 2007) because the geological cross sections and the results of logging (Fig. 2) are close for these two boreholes, although they are located quite far from each other (at a distance of 160 km). Generally, a section of these wells is composed of the sedimentary and volcanic-sedimentary complexes. The boundary between these two complexes, which is identified at a depth of 6424 m and 6921 m in the SG-

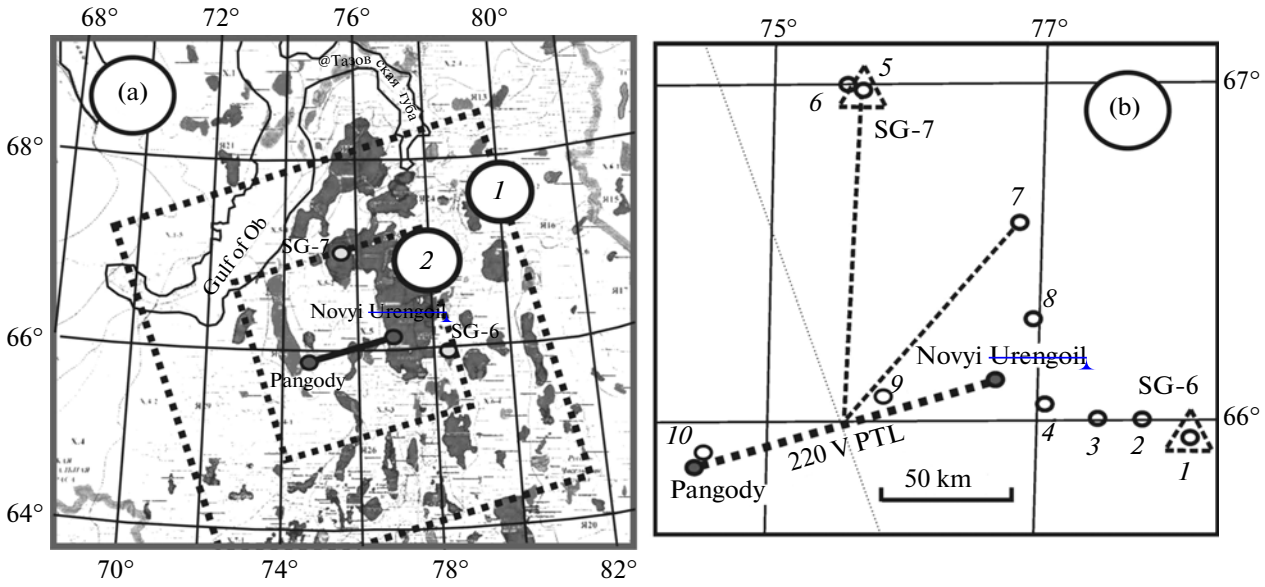

Fig. 1. The schematic map of the region of sounding: (a) the estimated contours of the regions covered by deep sounding with (a) Energiya-2 and (*2*) Energiya-3 generators connected to the Urengoi-Pangoda PTL. The dark spots mark the potentially gas-bearing areas; (b) the layout of the points of sounding in the field of the Urengoi-Pangody PTL with the connected Energiya-3 generator (*1*–*8*) and the locations of the SG-6 and SG-6 superdeep boreholes. Dots *9* and *10* indicate the AMT-MT sounding points.

6 and SG-7 wells, respectively, is marked by a sharp, almost tenfold increase in electric resistivity (Fig. 2). The uppermost portion of the section from the surface to a depth of 400 m is composed of alternating sandy and clayey interbeds of the Paleogene–Quaternary age. The SG-6 section contains a low-resistive layer (5–7 Ω m) at a depth of 200 m. This layer, although with a larger thickness, is identified in the section of SG-7 well at a depth of about 150 m. In the depth interval from 400 m to 1380 m, the electric resistivity of the rocks in the sections of both wells decreases in a wide interval from 20–30 Ω m to 2–3 Ω m. Geologically, this depth interval corresponds to the regional seal (fluid-resistive layer) composed of Paleogene–Upper Jurassic clays, which are poorly permeable for fluids and probably have low porosity, which is displayed in Fig. 2. Below this depth, in the interval from 1380 to 2700 m, there is a zone of porous reservoir rocks with an intergranular porosity of 15–20%, which can potentially contain gas accumulations. In the diagram of electrical logging, the interval of highly porous rocks is distinguished by the rise in electric resistivity up to 10–15 Ω m with increasing depth (Fig. 2). Below it, in the depth interval from 2.7 km to 4.3 km, the porosity decreases to 6–8%, while electric resistivity increases to 20–30 Ω m. The relationship between the electric resistivity and porosity of the rocks according to the logging data in the SG-7 hole has approximately the same but less pronounced character than in the SG-6 borehole.

Figure 2 and the description above demonstrate an untypical relationship between the electric resistivity and porosity in the upper part of the section. Here, the rocks have anomalously high porosity (up to 25%), while their electric resistivity steadily increases with increasing depth from 2–3 Ω m to 10–15 Ω m, although, according to the general physical considerations, the growth in the porosity should have been accompanied by the decrease in resistivity due to the increased percentage of highly conductive fluid in the rock. Attempting to explain this phenomenon, we suppose that the increase in porosity is accompanied by the reduction in the quality and number of channels connecting the pores and the capillaries. This, in turn, can result in the fact that the electrical resistivity of the rock overall increases with increasing porosity. However, the situation also admits an alternative interpretation. As porosity increases, resistivity can grow due to the increased content of the oil and gas mixture in the reservoir or due to the decreased concentration of salts in the electrolytic solution, which also leads to the increase in the electric resistivity of the rocks. We note that the mineral content of the pore water is 5.5 g/l, which corresponds to the resistivity of the water solution of about 1.5 Ω m (Dakhnov, 1955). Below 2.7 km, the resistivity and porosity are linked by the inverse relationship, i.e., the resistivity of the rock increases with decreasing porosity and vice versa according to the general physical regularities described in (Dortman, 1984). The experimentally established fact that the section contains an interval where a highly porous layer with high reservoir properties, which is more promising in the sense of its probable oil and gas capacity, corresponds to the zone of the increased electric resistivity, is the main result yielded by the electrical logging in the SG-6 and SG-7 wells. This, in

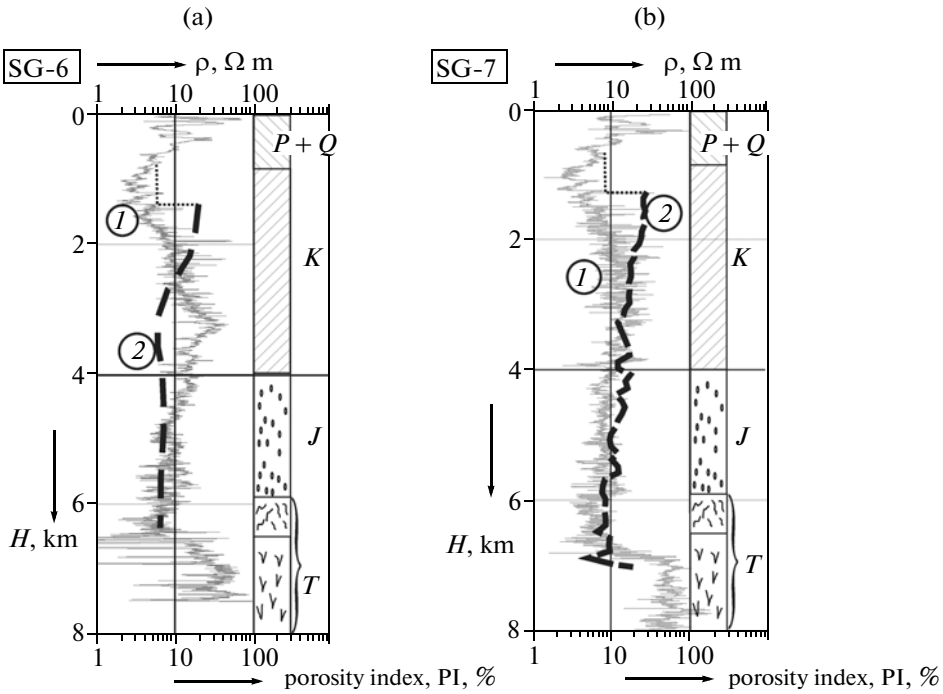

Fig. 2. The results of electrical logging in the (a) SG-6 and (b) (SG-7) superdeep boreholes (Tyumen and En-Yakhin, respectively) by the normal log (NL) technique. $P + Q$ stands for Paleogene-Quaternary rocks; K stands for Carboniferous; J stands for Jurassic; T stands for Triassic. The thin dashed line in curve 2 shows the lower boundary of the regional seal (fluid-resistive layer) composed of Paleogene-Upper Cretaceous clays, which are poorly permeable for fluids.

turn, indicates that, in combination with the other geophysical methods, deep electric prospecting is an efficient means for estimating the oil and gas bearing capacity of the sedimentary cover.

An important result of drilling the SG-6 and SG-7 boreholes is the retrieval of the data on the structure and presence of oil and gas in the effusive-sedimentary volcanogenic deposits below the sedimentary layer in the northern part of the West Siberian province. In its upper portion, the sequence of the Lower Triassic–Upper Permian effusive sedimentary strata is composed of intercalated fine-grained basalts and fused tuffs of the Korotchaevskaya Formation (6921–7078 m) with thin interbeds of cherty sedimentary rocks (silicites of Aimal Formation, 7078–7194 m). The similar situation is also observed in the section of the effusive rocks penetrated by the Tyumen SG-6 borehole (Gorbachev et al., 2007). In the interval from 7194 to 7418 m, the section is composed of basalts alternating with fused volcanic tuffs. Lower in the SG-7 section, layers of purely sedimentary rocks (claystone) occur up to a depth of 8248 m. Based on these facts, it was concluded that marine regimes in the accumulation of the volcanics of Permian–Triassic trap complex alternated with terrestrial regimes. The results confirm the regional character of the distribution of the effusive Triassic trap complex, whose upper part is composed by the tuff lavas and is underlain by thick basaltic strata. Alongside the low-capacity varieties of massive rocks, the trap complex also contains intervals of highly porous pore-fracture type reservoirs ($k_p = 15–20\%$). All this suggests that oil and gas accumulations are highly probable in the deep layers (below 5–6 km) in the territory of YaNAD, and that the gas and oil deposits can be hypothesized to recover, due to the transport of hydrocarbon gases from the underlying Paleozoic rocks (Esipko, Gorbachev, and Sokolova, 2000; Gorbachev et al., 2007). In the solution of these problems, it is reasonable to apply a complex of geophysical methods, including seismic prospecting and deep electromagnetic studies.

THE TECHNIQUES

The electromagnetic soundings were carried out in two stages. At the first stage (in 2011), we measured the ULF signals transmitted by the Zevs antenna, which is located in the Kola Peninsula (Velikhov et al., 1994), and carried out audio magnetotelluric and magnetotelluric soundings (AMT-MT) by measuring natural variations of the electromagnetic field in the region of the SG-6 and SG-7 wells. These works were codenamed NUR-2011. In 2012, we carried out testing frequency sounding measurements with the Urengoi-Pangody PTL by connecting the Energiya-2 generator (with a power of up to 200 kW) (June 2012) and Energiya-3 portable generator (with a power of 2 kW) (September 2012) to this electric line. In the description of the results of these studies in the present paper, we mainly focus on the soundings with the portable

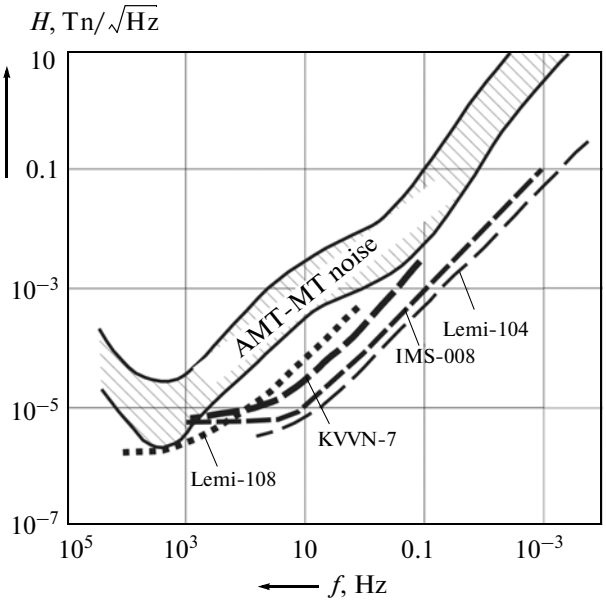

Fig. 3. The composite diagram showing the spectral characteristics of the self-noise of the induction sensors of the magnetic field (KVVN-7, IMS-08 and LEMI sensors) compared to the average noise level (the hatched band).

generator (codenamed NUR-2012, where NUR is the abbreviation for the name of the town of Novyi Urengoi). The results of the works of 2012, including the soundings with the Energiya-2 generator with a power of up to 200 kW, will be described in detail in our next paper.

In 2011, the signals of natural and controlled sources were recorded by the KVVN-7 seven-channel digital station (Kolobov et al., 2011). In order to improve the reliability of the measurements and to expand the frequency range, the magnetic field was measured by two sets of induction sensors simultaneously connected to five magnetic inputs of the station. Three sensors (*Hx*, *Hy*, *Hz*) designed at the Nizhny Novgorod Radio Physics Research Institute (NIRFI) are part of the KVVN-7 kit. Their frequency range is from 1000 to 0.1 Hz. In addition, we also used two IMS-008 wideband magnetic sensors (*Hx*, and *Hy*) designed by OOO VEGA. The frequency range of these sensors spans from 1000 Hz to 0.001 Hz. The noise characteristics of the both types of the sensors compared to the foreign LEMI magnetometers developed at the L'viv Centre of Institute for Space Research (Ukraine) (Korepanov et al., 2006) are shown in Fig. 3. It can be seen that the characteristics of the IMS-008 sensors throughout the entire frequency range lie below the level of natural noise (shown in Fig. 3 by the hatched band). The internal noise of the sensors of the KVVN-7 station at a frequency of about 0.1 Hz approaches the interval of natural noise and ceases to be suitable for reliably recording weak low-frequency MT variations.

The electric field was recorded by two nonsymmetric Γ-shaped grounded lines *MN* connected to the differential input of the station with a common ground. The length of the *MN* line varied within 300–500 m. The horizontal magnetic sensors and electric lines were oriented along the magnetic meridian (*Hx, Ex*) and magnetic latitude (*Hy*, *Ey*).

The Zevs transmitter (Fig. 4) includes two switch-generators of sinusoidal voltage, each with a power of 1 MW, and two parallel horizontal grounded antenna (which are the analogs of the grounded industrial PTL), each with a length of 55–60 km (Velikhov et al., 1994). The generators produce antenna current of up to 200–300 A in the frequency range from 40 to 200 Hz. The electromagnetic field of the Zevs source propagates in the Earth-ionosphere waveguide as a vertically polarized transversal electric TE-mode (Bernstain et al., 1974; Akindinov, Naryshkin, and Ryazantsev, 1976). This mode includes the longitudinal (parallel to the boundaries of the waveguide) horizontal component $H\varphi$ and the transversal vertical electric component *Ez*. The arrow *P* in Fig. 4 shows the direction of the Umov-Pointing vector. In accordance with the Leontovich boundary conditions, the $H\varphi$ component on the Earth's surface generates the electric field in the Earth; this field is oriented along the grounded current line AB (latitudinal component *Ey* in Fig. 4). Here, part of the energy is dissipated in the lower half-space in the form of a plane electromagnetic wave at $\lambda_0 \gg \lambda_з$, where λ_0 and $\lambda_з$ are the wavelengths in the air and in the Earth, respectively. The intensity of the horizontal field *Ey* is determined by the input impedance of the lower half-space Z_{erth} and the intensity of the field $H\varphi$ that arrives from the transmitter. On the surface of the Earth, component $H\varphi$ is denoted by *Hx*,

$$Ey = Z_з Hx, \text{ where } |Z_з| = \sqrt{\rho_з \omega \mu_0}.$$

By analyzing the input impedance on the surface of the layered lower half-space $Z_{\text{erth}} = Ey/Hx$ at different frequencies, one can carry out frequency sounding of the Earth in the field of the ULF antenna.

An important feature of the antennas of the Zevs transmitter in the Kola Peninsula is their location on the surface of a uniform poorly conductive block composed of granite-gneisses of an ancient protobasement (the Murmansk block). The effective electric resistivity ρ of the medium beneath the antenna is, on average, 5×10^4 Ω m. This means that at an average frequency of 100 Hz, the horizontal magnetic moment of the antenna $M = JLh_S$ attains 1.5×10^{11} A m^2, where *J* is the electric current intensity in amperes, *L* is the length of the antenna in meters, and $h_S = \sqrt{\dfrac{10^7 \rho}{f 8\pi^2}}$ is the skin depth beneath the antenna, which reaches 10 km within the Murmansk block. The timing of the main quartz-crystal oscillator was ensured by the Giatsint

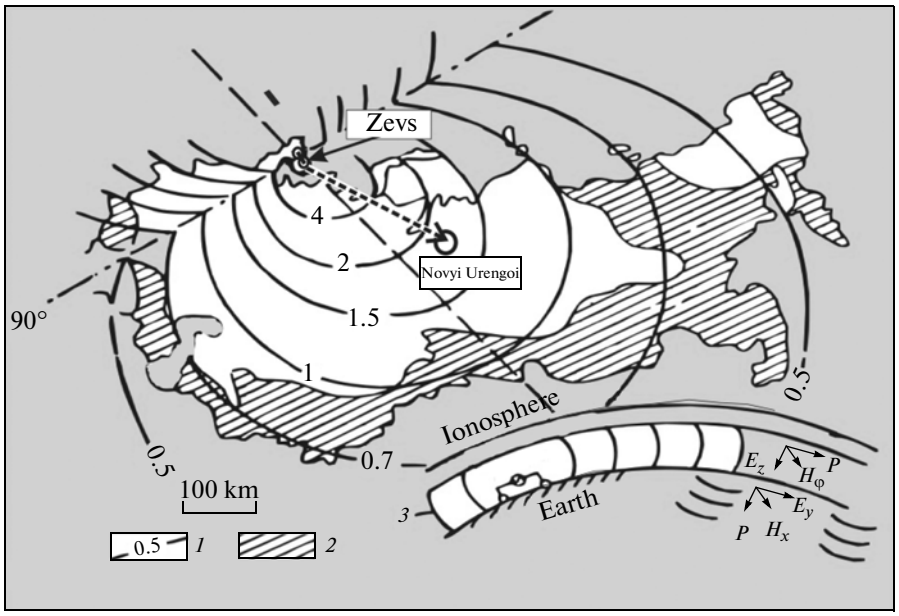

Fig. 4. The layout of the Zevs ULF antenna and the region of study (Novyi Urengoi): (*a*) the calculated isolines of the horizontal magnetic field H_{pgi} in nT at a frequency of 100 Hz and antenna current of 100 A; (*2*) the seismic hazard regions; (*3*) the schematic propagation of the ULF field in the Earth-ionosphere waveguide and in the lower half-space.

system with an accuracy of at least 10^{-7} s. During the experiment, according to the prescribed schedule, the Zevs transmitter was switched on at five frequencies: 41 Hz (195 A), 62 Hz (180 A), 82 Hz (215 A), 144 Hz (160 A), and 188 Hz (150 A) with a modulation time of 5–10 at each frequency (the numbers in the parentheses indicate the intensity of the electric current). The current in the Zevs antenna is sinusoidal at all frequencies. The theoretical isolines of the azimuthal magnetic component H_φ calculated in spherical coordinates at a frequency of 100 Hz and electric current of 100 A are shown in Fig. 4. The isolines of H_φ show that the region of study (Novyi Urengoi) falls in the favorable zone of the antenna pattern close to the axis of the source. The component $H\varphi$ in the region of Novyi Urengoi corresponds to the meridional component Hx in geographical coordinates. The radial electric component E_r, which corresponds to the latitudinal component E_y in the region of measurements (Fig. 4), has the same antenna radiation pattern. The field generated by the Zevs source according to the experimental observations is described in more detail in the next section.

THE RESULTS OF SIGNAL PROCESSING FOR THE TRANSMISSIONS BY THE ULF ZEVS ANTENNA

The recorded signals from the ULF Zevs source are shown in Fig. 5 in the form of power spectral density (PSD) diagrams for the electric and magnetic components of the field. The spectral processing of the signals was carried out by the Power Graph program. The signals were reliably recorded in the region of both boreholes by both sets of the induction sensors of KVVN-7 and IMS-008 with an identical error. In the region of the SG-6 superdeep borehole, the noise level is significantly higher than that in the region of SG-7 borehole, particularly in the electric field. The fact that the noise level in the electric field strongly exceeds the noise level in the magnetic field in the region of SG-6 indicates that the noise has a galvanic origin. As a result, this reduces the coherence between the conjugated components of the electromagnetic field of both natural and artificial origin.

By examining Fig. 5, we see that the *Ey* and *Hx* components strongly exceed *Ex* and *Hy* at both measurement sites. This behavior of the field agrees with the theory which predicts that the field of a long grounded current line in the zone that is predominantly controlled by the ionosphere and displacement currents are elongated along the axis of this line (Bernstain et al., 1974; Akindinov, Naryshkin, and Ryazantsev, 1996). The PSD diagrams (Fig. 5) show that the signal intensity of the magnetic field barely changes with increasing distance to the source; moreover, the electric signals in the zone of the SG-6 borehole are even stronger (by 30%) than those in the zone of SG-7 which is located 160 km closer to the source. This behavior of the field is reasonably accounted for by the higher electric resistivity of the upper layers of the section in the region of SG-6 (Fig. 2). The full amplitude of the recorded signals in Fig. 5 can be estimated directly from the graphs of PSD in the following way:

$$E = \sqrt{\text{СПМ}_E \Delta f}, [\text{V/m}] \text{ and } H = \sqrt{\text{СПМ}_H \Delta f}, [\text{A/m}].$$

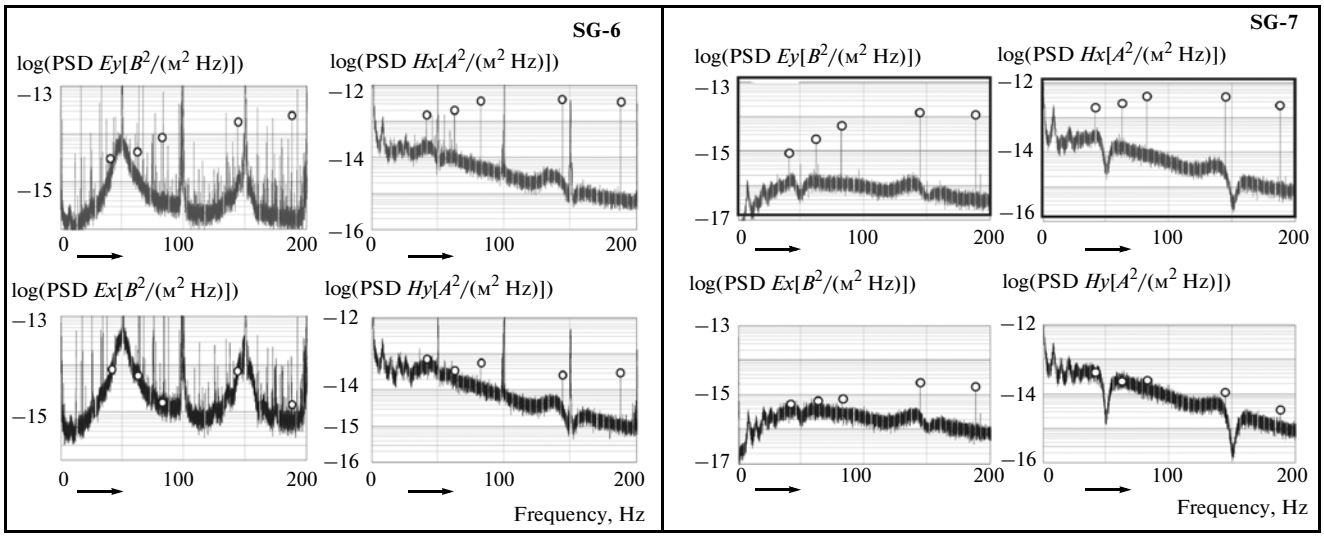

Fig. 5. The power spectral density (PSD) diagrams of the electrical and magnetic field according to the Zevs ULF signal recording in the region of SG-6 and SG-7 boreholes. The amplitudes of the signals transmitted by Zevs are shown by the circles at the corresponding sounding frequencies. The location of the Zevs source and the points of signal recording is shown in Figs. 1 and 4.

The sampling frequency Δf is 0.002 Hz; therefore, it can be easily determined from the graphs that the average recorded intensities of the main components of the field range within 2–12 μV/km for *Ey* and 32–66 fT for *Hx*.

The signals generated by the ULF Zevs antennas and the variations of the natural AMT-MT field were independently processed by two teams of scientists. In this section, we present the results of processing by the program developed by A.N. Shevtsov (2006). The processing is conducted by the Walsh method based on the fast Fourier transform (FFT) with different windows and overlapping segments of a record. Before processing, the records, which were initially sampled at a frequency of 5 kHz, were decimated to a frequency of 500 Hz. The window that is optimal in terms of frequency resolution and statistical stability of the obtained estimates, which ensures a 40% overlapping of the fragments of a record, is obtained for a sampling frequency of 500 Hz with 2^{18} samples. The Blackman-Harris window was used as the weighting function. The estimates of PSD were calculated for each component, and the cross PSD were calculated for each pair of components. These estimates were used for calculating the partial coherences and transfer functions (impedances) (Semenov, 1985). On the basis of these values, the apparent resistivities (ρ_T) and the phase shifts between the components of the field (the impedance phases) at the given frequencies were determined. For further processing, representative resistivity and impedance phase values were selected by the criterion of coherence: the geometrical mean of the coherences for the collinear components of the electric and magnetic field should be at most 0.4, and the geometrical mean of the coherences of mutually orthogonal components of the electric and magnetic field should be at least 0.6.

The processing results for the soundings with natural and controlled sources are shown in Fig. 6 and marked by numbers 1, 2, and 3 in the circles. The solutions of the forward problem for the geoelectrical cross sections according to the well logging data in SG-6 and SG-7 boreholes are also shown in this figure by the dashed lines marked by number 3 in the circle. We note that the forward problem is solved for the cross sections reconstructed from the longitudinal electric resistivity ρ_l. The ρ_l curves for SG-6 and SG-7 are calculated from the logging data for the electrical current that flows horizontally along the predominant bedding of the rocks, which corresponds to the induction (poloidal) excitation of the secondary field in the far (plane wave) zone of both the natural and controlled sources (Vanyan, 1965). The values of ρ_l were determined by recalculating the well logging data with a varying interval of averaging. In the uppermost layers of the section (above 80 m), where the reliable logging data are absent since the diameter of the borehole is 720 mm and the results of measurements mainly reflect the effect of the electrically conductive drilling fluid, the average resistivity of the section is assumed to be 70 Ω m for SG-7 and 100 Ω m for SG-6. In the depth interval from 80 m to 500 m, the averaging interval is 20 m. Below 500 m up to the borehole's bottom, the averaging interval is 100 m. The conversion to longitudinal resistivity was carried out by the following algorithm:

$$\rho_{li} = \frac{\Delta Z}{\Delta S_i}, \text{ где } \Delta S_i = \int_{Z_i-0.5\Delta Z}^{Z_i+0.5\Delta Z} \frac{1}{\rho_k(Z)}\delta Z;$$

ΔZ is the averaging interval (20 or 100 m), Z_i is the depth to the center of the current averaging interval, $\delta Z = 2$ m is the sampling interval of $\rho_k(Z)$ along the depth in the logging diagram, and Z is the depth corresponding to the current sample.

The sections of longitudinal electric resistivity calculated from the logging data are shown in Fig. 6. The corresponding theoretical curves of apparent resistivity and impedance phase calculated by solving the forward problem are marked by the number 3 in the circle in Fig. 6.

The apparent resistivity estimated from the measurements of the field generated by Zevs is denoted by the number 1 in the circle in Fig. 6. We note that the values of apparent resistivity of the Zevs source can be directly estimated from the PSD diagrams presented in Fig. 5 by the following formula:

$$\rho_T = \frac{|Z_{yx}|^2}{\omega\mu_0} = 0.127T\frac{\mathrm{PSD}_{Ey}}{\mathrm{PSD}_{Hx}} \times 10^6, [\Omega\,\mathrm{m}].$$

The apparent resistivity calculated in this way closely agrees with the data of statistical processing (1 in Fig. 6). The general analysis of the results in Fig. 6 shows that in the low-noise region (SG-7 borehole), the telluric (AMT-MTS) and controlled-source soundings reasonably agree with each other and with the logging data. In the region of high industrial noise (SG-6), the AMT-MT soundings exhibit a wide scatter, whereas the results of the controlled-source sounding with Zevs transmissions at high frequencies (188–82 Hz) demonstrate a close agreement with the logging data. Only at the two lower frequencies (62 Hz and 41 Hz), are the values of the apparent resistivity in the zone of SG-6 borehole shifted to the high frequency interval due to the influence of noise.

THE RESULTS OF PROCESSING AND INTERPRETATION OF AMT-MT DATA

Figure 7 shows the hodographs of the ends of the electric and magnetic field vectors of natural AMT–MT variations during the interval of signal recording at four measurement points (about 40 min). At points 1, 9, and 10, the electric field is polarized linearly, and only at point 5, the electric field has an elliptic, close to circular polarization, which is favorable for AMT processing. In contrast to the electric field, the magnetic field at all observation points is polarized elliptically. In Fig. 7a, the locations of the axes of the linear polarization of the electric field are correlated to the scheme of the age of the Paleozoic crust (Aplonov, 2000), where the location of the axial line of the Ob' paleorift and the transform faults are indicated. According to this scheme, point 1 falls in the zone of a complex tectonic junction, and the polarization direction of the electric field coincides with the strike of the transform fault. Points 9 and 10 are located west of the rift axis, and the electric field here is polarized subparallel to the strike of the rift. Although point 5 is located in the same conditions as points 9 and 10, the electric field here is not linearly polarized. Remarkably, among the soundings in the region of SG-6, a particularly sharp linear polarization of the electric field was observed during repeated sounding 1a. This can be probably due to the changes in the location of the noise source (the measurements were carried out at different times of the day) or to the specific technical features of the record. Therefore, processing was carried out for the first interval of measurements (on September 23). However, even this processing did not provide stable results. The general analysis of the results shows that the MT-AMT data processing in the one-dimensional approximation is only possible for point 5 located close to the En-Yakhin superdeep well SG-7.

In the region of this borehole, as it has been mentioned above, the industrial noise is lowest (Fig. 5). The AMT-MT data were processed by the PTS original program developed by a group of authors (M. ~~Petrischev,~~ A. Tkachev, and V. Semenov). In the processing, the correlation between the spectra of the components of electromagnetic field was estimated by the coherence level (Semenov, 1985), and the directions along which the diagonal elements of the resistivity tensor were absent or negligible were selected. Once this direction was established, the data were analyzed by sliding along the record in order to accumulate a statistical set of the estimates. The sliding was carried out with the specified thresholds of coherence, which lowers the displacement error in the determination of the main and additional impedances. Then, in the obtained set of apparent resistivity values, the median estimates were determined for each period. The advantage of this approach is that the random error decreases in this case.

The obtained MT curves can be complemented by the results of magnetovariational sounding carried out at the nearest observatory, for which the complex apparent resistivity curve is known. This approach significantly increases the stability of inverse problem solution by conducting the corresponding inversions; moreover, in many cases, it eliminates the displacement errors due to the static shift of the apparent MT resistivity at long periods. In practice, the D+ (Parker, 1980) and OCCAM (Constable, Parker, and Constable, 1987) inversions are very efficient. The first inversion places emphasis on the estimation of the modulus of apparent resistivity, whereas the second one is mainly focused on estimating its phase. The analysis of the data for the zone of SG-7 borehole shows that OCCAM inversion is preferable because the errors in estimating the phase are mainly controlled by the random error, whereas the errors in the estimates of the modulus are associated with both the random errors and the static shift.

The results of the interpretation are shown in Fig. 8. The interpretation is carried out for E polarization whose azimuth was about 30 degrees west. Along

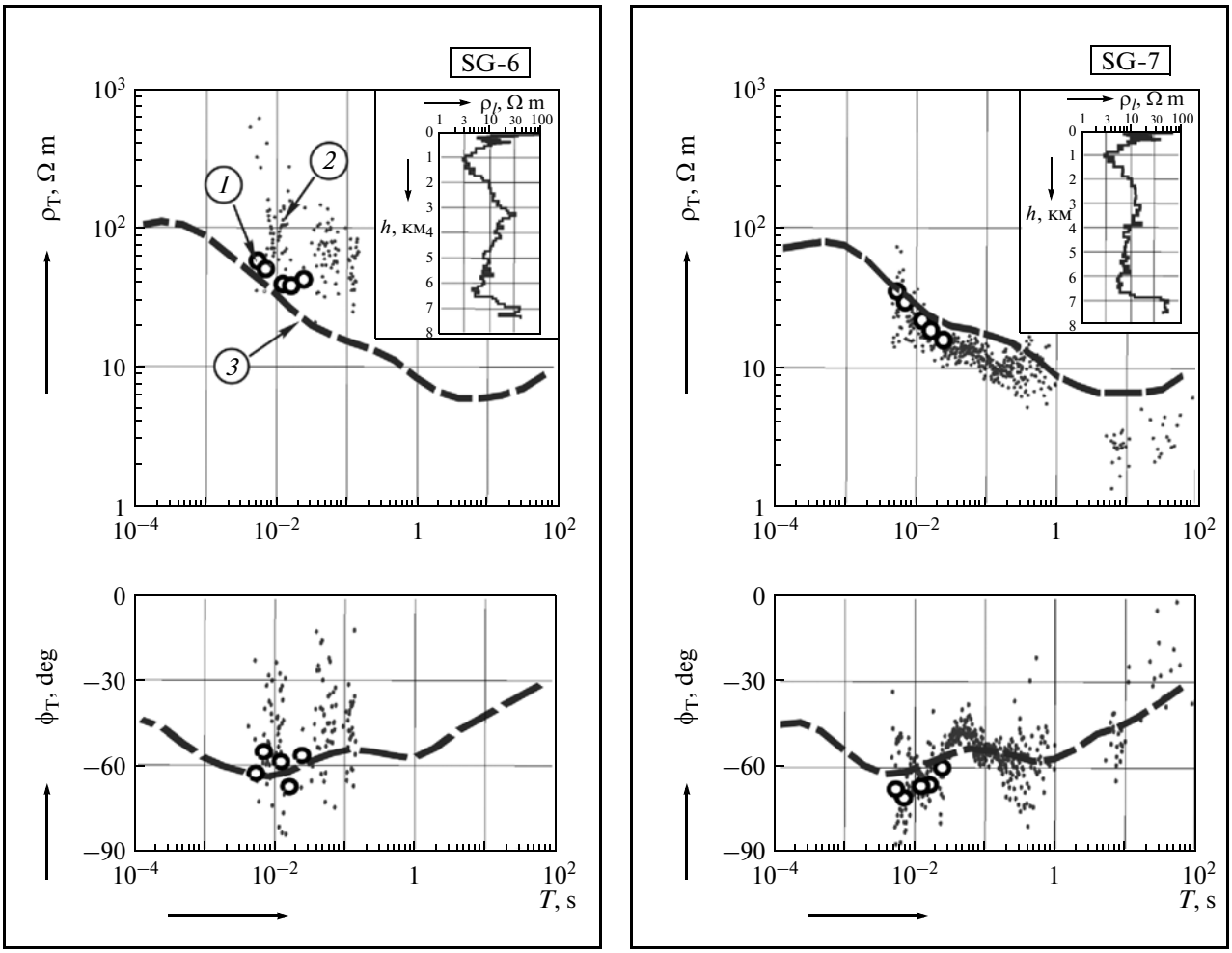

Fig. 6. The composite diagrams of apparent resistivity according to the (*1*) Zevs signal processing data and (*2*) AMT-MT soundings in comparison with the (*3*) solution of the AMT-MT direct problem for the geolelectrical logging sections of SG-6 and SG-7 boreholes. The sections for SG-6 and SG-7 boreholes are shown in the right top corners of the corresponding diagrams.

this direction, stable response functions are obtained in the period range from 10^{-3} to 10^2 (the circles 2 in Fig. 8a). This direction, which is shown by the number 5 in Fig. 7a, corresponds to the axis of the Ob' paleorift (Aplonov, 2000). The results of the MT sounding were complemented by the response function at the nearest observatory in Novosibirsk (NVS) in the period range from 4×10^5–10^8 s (Semenov and Kharin, 1997), in the same way as it is done in (Semenov et al., 2008). The gap between these intervals was partly covered by the results of the numerical modeling on the sphere, which was carried out by Yan ~~Vosar~~ by the program of A.V. Kuvshinov (Kuvshinov et al., 2005) for the NVS observatory according to the procedure described in (~~Vosar~~ qand Semenov, 2010).

After this, the data were inverted by two well-known algorithms, namely, the D+ (Parker, 1980) and OCCAM inversions (Constable, Parker, and Constable, 1987). The D+ inversion implements the algorithm, which is suitable for creating geoelectrical media with a finite number of layers having zero thickness and finite electric conductivity, which are separated by ideal insulators (Parker, 1980).

The one-dimensional (1D) OCCAM inversion is based on the algorithm described in (Constable, Parker, and Constable, 1987). Here, by applying the least square method $X^2 = \sum_{j=1}^{M} \frac{(d_j - F_j[m])^2}{\sigma_j^2}$ to the data d_j and the presumed root mean square deviations σ_j^2, one searched for the flattest model of the medium m by minimizing the first $R_1 = \int \left(\frac{dm}{dz}\right)^2 dz$ or second derivative.

The inversion of the obtained sounding curves with different parameters carried out by the MTID v.2.0 program yielded the model of the geoelectrical section (8) shown in Fig. 8b. The results of the resistivity logging in SG-7 well (normal log) (6) and lateral logging (7) are also displayed in this figure. The solution of the

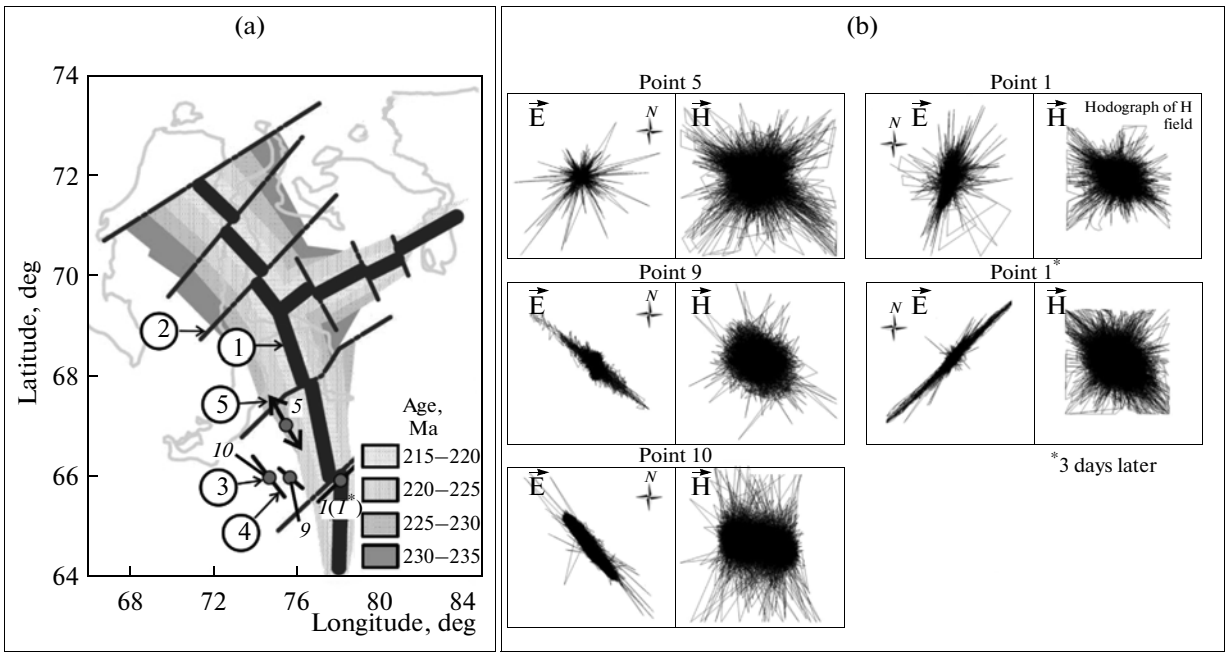

Fig. 7. (a) The position of the AMT sounding points on the schematic age map of the Paleozoic crust (Aplonov, 2000) and (b) the hodographs of the vectors of electrical (*E*) and magnetic (*H*) field in the sounding points. The numbers in the circles indicate the following elements: *1* the axis of the Ob paleorift; *2* the axes of the transform faults; *3* the points of MT-AMT sounding; *4* the linear polarization axes of the electrical field; *5* the selected principal direction of the ~~tensor~~ impedance matrix at point *2* located in the zone of SG-7 borehole.

inverse problem (8 in Fig. 8b) is shown as the hatched band whose width corresponds to the confidence interval. According to the results of the sounding in the SG-7 well, two conductive layers are identified in the upper part of the section (Fig. 8b). The curve of the geoelectric section here closely agrees with the logging data, but it is shifted towards the higher resistivity values. The first conductive layer occupies a depth interval from 150 to 200 m and has a resistivity of about 10–20 Ω m (7–8 Ω m according to the logging data). The second layer, which is thicker, is located at a depth from 500 m to 2000 m and has a resistivity 6–7 Ω m (3–5 Ω m according to the logging data). The logging data and the geoelectrical curve somewhat diverge in the interval from 6 to 7 km (5–20 Ω m according to logging against 150–200 Ω m in model 8). This divergence is probably caused by the lower quality of the experimental data in the long-period interval (a few dozen seconds) and poor resolution of the method to the deep, thin weakly contrasting layers. Below 7 km, where a thick layer of low-conductive basalts begins, the results of logging and MTS again closely agree. In the lower part of the section, at a depth of 10–12 km, there is a stepwise transition from the poorly conductive trap basalts (150–200 Ω m) to the even less conductive rocks of the middle crust where the resistivity exponentially grows up to a few thousand Ω m due to the reduced porosity and fluid content in the crystalline rocks. Starting from a depth of 20–30 km, the crustal resistivity exponentially decreases due to the increase in temperature with increasing depth. In the interval from 250 to 400 km, an intermediate conductive layer, which is presumably associated with the asthenosphere, is seen.

THE SOUNDING IN THE FIELD OF THE URENGOI-PANGODY PTL

The frequency soundings in a wider interval (0.38–175 Hz), compared to the Zevs transmissions (41–188 Hz), were conducted using the Urengoi-Pangody industrial PTL, which has a length of 114 km (Fig. 1). Alternating current was provided by the Energiya-2 generator supplying a power of 200 kW and by the Energiya-3 portable generator, which has a power of 2 kW. Test experiments with the high-power Energiya-02 generator showed that it can generate the electric current with the intensity of up to 100–120 A in the frequency range from 0.05 to 188 Hz in the industrial PTL. The procedure and results of these measurements will be described in our next paper. In this section, we present the techniques and results of the measurements with the portable 2-kW Energiya-3 generator. The expediency and necessity of constructing a portable generator and conducting the testing-methodical measurements with its use were dictated by a number of technical and logistical factors. Among them are the simplified scheme of connecting the Energiya-3 portable generator to the auxiliary power sources and to the PTL itself (by the 220-V network),

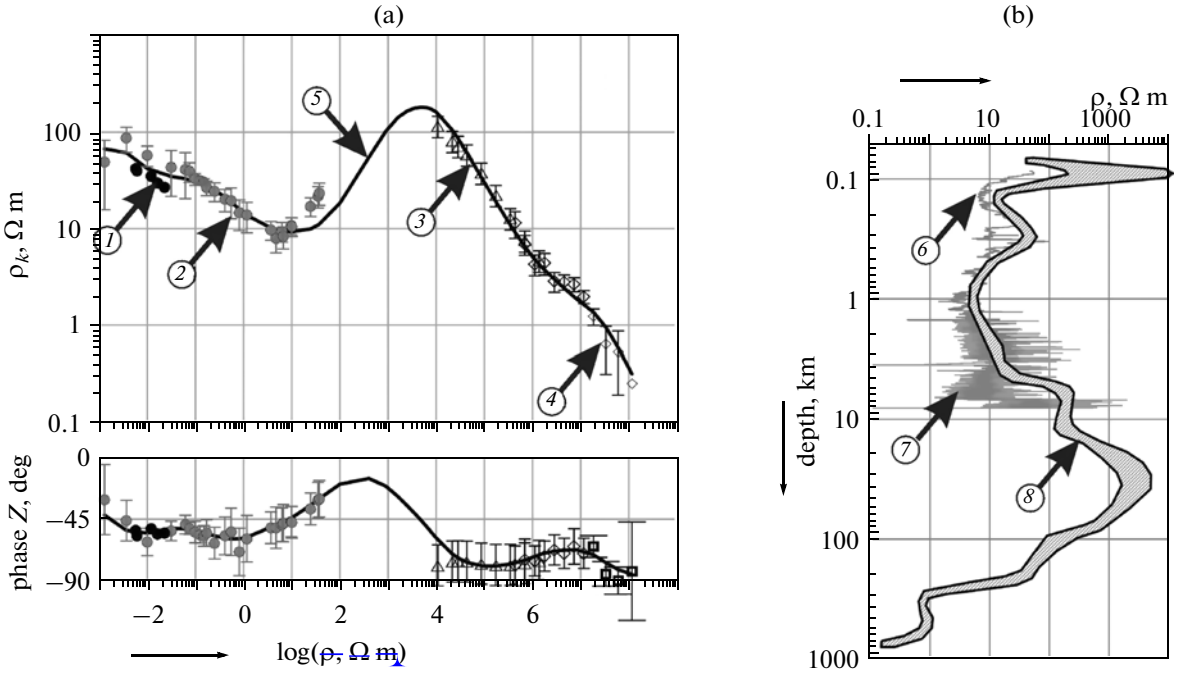

Fig. 8. The results of the NUR-2011 experiment on electromagnetic sounding in the region of the superdeep SG-7 borehole using the natural fields and the field of the ULF Zevs antenna: (*a*) the composite diagram of the apparent resistivity curves and impedance phase; (*b*) the comparison of the inverse problem solution with the logging data. The numbers in the circles show the following elements: *1* the soundings in the field of the ULF Zevs antenna; *3* AMT-3MT soundings; *3* deep Magnetovariational sounding (DMVS), Novosibirsk; *4* global data; *5* model curve according to the inversion; *6* and *7* logging data (*6* normal log, *7* lateral log); *8* geoelectrical cross section according to the inversion of MTS-AMTS-DMVS data and Zevs soundings.

the optimal electromagnetic connectivity of the current of the portable generator with the communication lines and with the underground utility lines, and the low weight–size parameters, which ensure easy and prompt transportation of the generator to the measurement site. Suffice it to say that the weight of the Energiya-3 portable generator, which can generate an electric current of up to 10–12 A in the Urengoi-Pangody line, is 10 kg. The similar parameters of the Energiya-2 generator are 100-120 A with a weight of 1000 kg. The necessity to use a certain type of generator depends on the particular objectives of the experiment and on the required spatial range of the observations. The recommended areas of deep electromagnetic soundings with the Energiya-2 generator (contour 1 covering an area of about 200000 km^2) and the Energiya-3 portable generator (contour 2 covering an area of about 40000 km^2) are shown in Fig. 1a.

The structural schematic of the portable ULF-ELF Energiya-3 generator and the pattern of its connection to the Urengoi-Pangoda PTL are shown in Fig. 9. The generator is based on the output inverter (OI), which forms the sine electric current with arbitrary amplitude and frequency in PTL. The formation of the output sinusoidal electric current implements the principle of pulse-width modulation (PWM), which is considered in detail in (Barannik et al., 2009). If necessary, the output waveform of OI can be changed into an arbitrary form (meander, triangle). The matching unit (MU) compensates the inductance of the complex impedance of the line at frequencies above 10 Hz, when the reactance of the line starts limiting the intensity of the electric current in the antenna. The capacity of MU upon the transition from one generation frequency to other changes in such a way as to always maintain the voltage resonance in the inductive load. At high operation frequencies when MU is used, OI forms a meander-shaped (rectangular) output signal so that the sine waveform of the current in the line is independently ensured by the resonance. In the case of operation at low frequencies when there is no need to use MU, OI outputs a sine waveform.

The electromagnetic field of the portable Energiya-3 generator connected to the Urengoi-Pangody PTL was measured by two identical VMTU-10 stations, which were developed by VEGA (Kopytenko et al., 2010), at eight measurement points installed along the roads approximately in the sublatitudinal and submeridional directions (Fig. 1b) At each point, the diurnal recording of AMT-MT field and the DC soundings with lines of up to 500 m were also carried out. The example of recording the signals of PTL at points 5 and 7 located at distances of 87 and 100 km from the midpoint of the line is shown in Fig. 10. At a distance of 100 km, the electric field was measured by a symmetrical MN line 1 km in length. It can be seen that the signals in PTL are reliably recorded up to 3.8 Hz in both the electrical and magnetic components. It

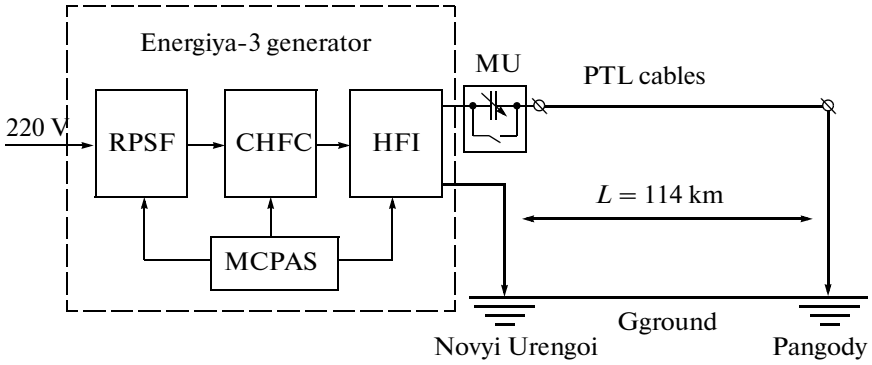

Fig. 9. The schematic diagram of the 2-kW Energiya-2 generator and the pattern of its connection to the 220-V electrical source and contour groundings of the end stations of the Urengoi-Pangody industrial PTL by the ground wire scheme. RPSF is rectifier and power supply filter; CHFC is controlled high-frequency converter; HFI is high-frequency inverter; MCPAS is the monitoring, control, protection and automatics scheme; MU is the matching unit; SPB is the surge protection block.

is remarkable that the amplitude of the field insignificantly varies with increasing distance between the source and the receiver. Our calculations show that this is mainly accounted for by the different geometry of the soundings and, at the highest frequencies, partly by the influence of the ionosphere.

Figure 11 illustrates the results of processing frequency soundings with the Energiya-3 portable generator in the field of the Urengoi-Pangody PTL, which were carried out in the region of SG-7 in 2012 (Fig. 1b). It is seen that the apparent resistivity measured in the field of two different types of the controlled sources, which are located at distances of 110 km (Urengoi-Pangody PTL, measurements carried out in 2012, shown by circle 1 in Fig. 11a) and 2000 km (Zevs transmitter, measurements of 2011, circle 2 in Fig. a1b) from the measurement point, closely coincide and agree with the theoretical apparent resistivity curve calculated with the logging data in the SG-7 well (circle 6 in Fig. 11a) taken into account. The MT results visualized in the form of a cloud of apparent resistivity values (marked by circle 3 in Fig. 11a) follow the shape of the theoretical curve 6, although with a downward shift along the resistivity axis by almost half an order of magnitude. We note that the results of MT soundings carried out in 2011 shown in Fig. 8 in the same frequency band are located by an order of magnitude higher. This is associated with the particular features of the procedure of MT data processing. In 2011, the coordinate system was rotated to the direction in which the diagonal components of resistivity tensor are negligible. This direction was 30 W, and the obtained apparent resistivity curve was close to the effective (i.e., maximal) curve. In 2012, all the soundings with natural and controlled sources were processed for the same pair of the electromagnetic components oriented along the magnetic meridian (magnetic field) and latitude (electric field), which correspond to the optimal orientation of the controlled-source fields used in the experiment.

The soundings of 2012 were processed by a methodically improved inversion procedure. In this procedure, largest weights were imparted to the controlled-source soundings at the shortest periods (circles 1 and 2 in Fig. 11a) and to the geomagnetic responses of the natural fields at the longest periods (deep magnetovariational soundings, DMVS, circles 4 and 5 in Fig. 11a). As known, the soundings in the MT range of periods are most prone to static distortions, which result in the displacement of the apparent resistivity curve. The phase curve is free of this influence; however, this curve requires quantitative referencing to the level of apparent resistivity. The improved algorithm of the inversion solves this problem by referencing it to the high-frequency (AMT) and low-frequency (MT) branches of the curves of deep sounding, as mentioned above.

The comparison with the experimental data of 2011 (Fig. 8) demonstrates the noticeable advantage of the new results which take into account the data of soundings with the Energiya-3 portable generator and rely on the new processing algorithm. The fitted section (circle 9 in Fig. 11b) closer agrees with the results of resistivity logging (circle 8 in Fig. 11b). Here, it is important that the model apparent resistivity curve (6 in Fig. 11a) is displaced upwards relative to the experimental MT curve (3 in Fig. 11a). This shift is probably associated with the regional features of the magnetotelluric field, which appeared due to one-dimensional processing of the data, and, partly, with static shift.

CONCLUSIONS

Our results demonstrate the wide possibilities of the complex electromagnetic soundings with medium- and high-power natural and controlled sources in studying the deep structure of the sedimentary cover within the oil- and gas-bearing territories of the Yamal-Nenets Autonomous District. The controlled-source soundings can be conducted in the fields gener-

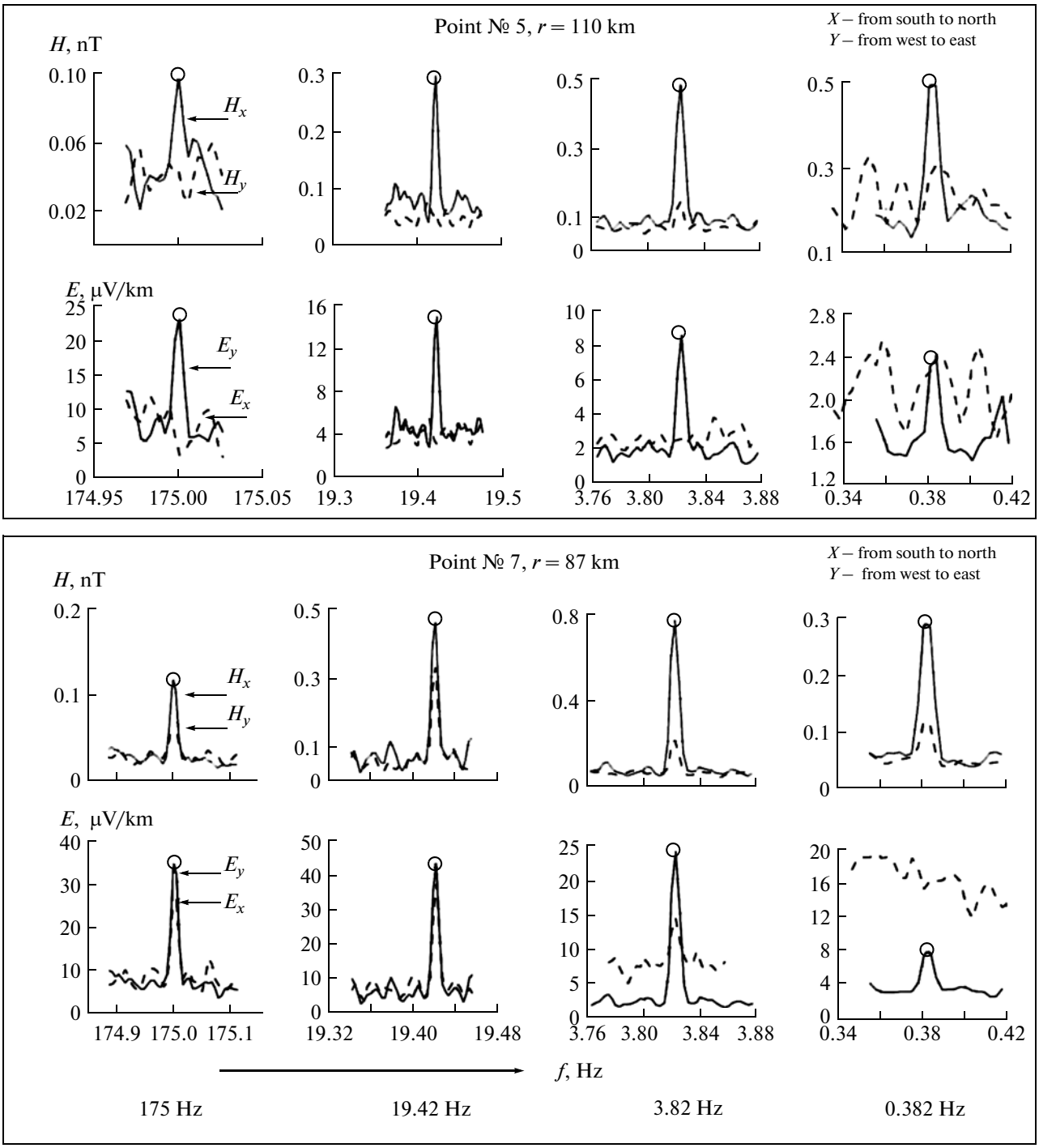

Fig. 10. The amplitude spectra for the electrical and magnetic fields according to the data of the experiment on recording the signals of 2-kW portable generator connected to the 220-V Urengoi-Pangody electric line. The measurements are carried out at points *5* and *7* located at a distance of 100 and 87 km from the center of PTL, respectively. The layout of the sounding points is shown in Fig. 1b.

ated by the ULF Zevs antenna, which uniformly covers the entire territory of YaNAD, or relatively local fields of the industrial electric lines with generators, which output medium or high power depending on the goals of the study, temporarily connected to them. The main advantages of the soundings with fixed controlled sources is that they provide (a) highly unambiguous solutions of the inverse problem since the parameters of the source are a priori known, (b) the controllable accuracy of the results, and (c) the wide

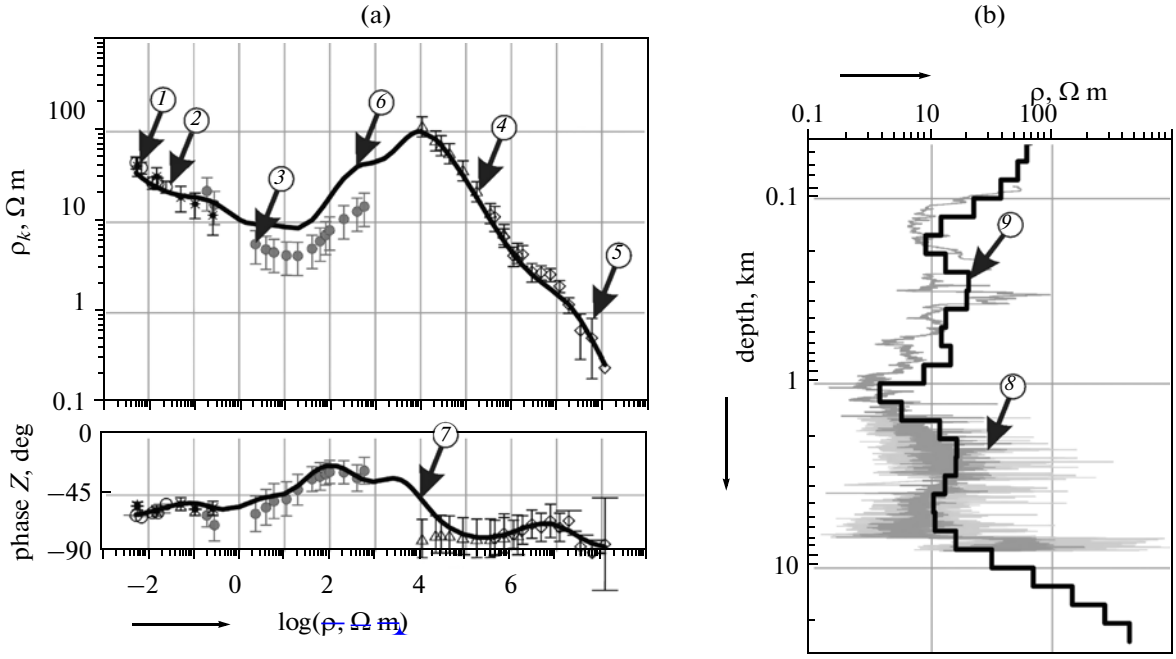

Fig. 11. The results of the NUT-2012 experiment on the deep sounding with the (*1*) portable Energiya-3 generator and industrial Urengoi-Pangody PTL in combination with the (*2*) Zevs source, (*3*) AMT-MT soundings, and (*4, 5*) DMVS. The left diagram (*a*) shows the apparent resistivity and phase curves; the right diagram (*b*) shows the geoelectrical cross sections according to the (*8*) logging data and (9) sounding data; *4* is the curve of DMVS in Novosibirsk; *5* is the global data; *6* is the model curve for the inversion of the modulus of apparent resistivity; *7* is the same for the impedance phase inversion; *8* the normal-log data for SG-7 borehole; *9* the geoelectrical section yielded by the joint inversion of the natural-source soundings (MT = -AMT-DMVS) and controlled-source soundings (ULF Zevqa antenna, portable Energiya-3 generator connected to the Urengoi-Pangody industrial PTL).

possibilities of signal filtering against natural and industrial noise. The advantages of soundings with natural sources (AMT and MT soundings) mainly lie in the low-frequency range (below 1 Hz). The average intensity of the variations in the natural electromagnetic field in this frequency range sharply increases with decreasing frequency, whereas in the case of accumulation of signals from the controlled sources, the necessity to sharply increase the interval of current generation arises. Another advantage of the AMT-MT soundings stems from the fact that it automatically provides the fulfillment of the far-zone condition (the plane wave approximation), which is not always valid in the soundings with the controlled sources. The exception is the field generated by the ULF Zevs antenna, since this facility has a unique power and almost infinite range of radiation.

ACKNOWLEDGMENTS

This work is supported by the Russian Foundation for Basic Research (grant no. 11-05-12033-ofi-m-2011 led by Dr. Sci. A.A. Zhamaletdinov) and grant 6 from the Department of Earth Science of the Russian Academy of Sciences (led by Acad. A.B. Gliko and F.P. Mitrofanov). We are grateful to V.Yu. Semenov for his valuable comments on the techniques of data processing and interpretation; Jan Vozar for providing the results of the numerical modeling of the response function at the NVS observatory; and A.A. Petrova for discussing the results on the modeling of magnetic anomalies. We are also grateful to V.V. Plotkin for reviewing our manuscript and his valuable comments, which were taken into account by the authors. Great help in processing the data and preparing the manuscript was provided by T.G. Korotkova, principal programmer at the Geological Institute of Kola Science Center of Russian Academy of Sciences. We are particularly grateful to the YaNAD Governor D.N. Kobylkin for his support, Dr. Sci. (Phys.-Math.) Yu.G. Schors, the officials of the Administration of YaNAD I.V. Petrova and A.L. Titovskii, and the management of the Yamal-Nenets Enterprise of the Main Electric Networks of Western Siberia for organizing the support for our work and providing the Urengoi-Pangody PTL as the antenna for conducting our experiments.

REFERENCES

Akindinov, V.V., Naryshkin, V.I., and Ryazantsev, A.M., Electromagnetic fields in seawater (A review), *Radiotekh. Elektron.*, 1976, vol. 21, no.5, 99.913–944.

Aplonov, S.V., *Geodinamika glubokikh osadochnykh basseinov* (Geodynamics of Deep Sedimentary Basins), St. Petersburg: TsGI TETIS, 2000.

Berdichevsky, M.N., *Elektricheskaya razvedka metodom magnitotellurichеskogo profilirovaniya* (Electric Prospecting by Magnetotelluric Profiling Method), Moscow: Nedra, 1968.

Bernstein, S.L., Burrows, M.L., Evans, J.E., Griffiths, A.S., McNeill, D.A., Niessen, C.W., Richer, I., White, D.P., and Willim, D.K., Long-range communications at extremely low frequencies, *IEEE Proc.*, 1974, vol. 62, no. 3, pp. 292–312.

Constable, S.C., Parker, R.L., and Constable, C.G., Occam's inversion: a practical algorithm for the inversion of electromagnetic data, *Geophysics*, 1987, vol. 52, pp. 289–300.

Dakhnov, V.N., *Elektricheskaya razvedkm neftyanykh i gazovykh mestorozhdenii* (Electric Prospecting for Oil and Gas), Moscow: Gostoptekhizdat, 1953.

Dortman, N.B., *Fizicheskie svoistva gornykh porod i poleznykh iskopaemykh (spravochnik geofizika)* (Physical Properties of Rocks and Minerals), Moscow: Nedra, 1984.

Esipko, O.A., Gorbachev, V.I., and Sokolova, T.N., Physical properties of the rocks from the Tyumen Supedrdeep Borehole from Geophysical Data, *Geol. Geofiz.*, 2000, vol. 41, no. 6, pp. 905–919.

Gorbachev, V.I., Tarkhanov, G.V., Esipko, O.A., Parasyna, V.S., Kovalenko, V.S., Marinin, V.I., and Konanykhin, G.A., The results of drilling the En-Yakhin superdeep borehole, in *VII Koordinatsionnoe geologicheskoe soveshchanie* (The 12th Coordinating Geological Meeting), Moscow: OOO IRTs Gazprom, 2007, pp. 183–193.

Ingerov, O.I., Modern trends in the development of instrumentation for land and marine electrical prospecting. A Lecture, in *Materialy 5-i Vserossiiskoi shkoly EMZ-2011* (Proc. of 5th All-Russia Workshop on Electromagnetic Sounding of the Earth (EMS 2011)), St. Petersburg, Petrodvorets: SPbGU, 2011, pp. 86–103.

Khakhaev, B.N., Gorbachev, V.I., Bochkarev, V.S., et al., Main results of superdeep sounding in the West Siberian oil- and gas-bearing province, in *Fundament, struktury obramleniya Zapadno-Sibirskogo mezozoisko-kainozoiskogo osadochnogo basseina, ikh geodinamicheskaya evolyutsiya i problemy neftegazonosnosti* (The Basement, the Margin Structures of West Siberian Mesozoic-Cenozoic Sedimentary Basin, Their Geodynamical Evolution and the Problems of Oil- and Gas-Bearing Capacity), Tyumen–Novosibirsk, 2008, pp. 224–227.

Kolobov, V.V., Kuklin, D.N., Shevtsov, A.N., and Zhamaletdinov, A.A., The KVVN-7 Multifunction Digital Measuring Station for Electromagnetic Monitoring of Seismoactive Zones, *Seism. Instrum.*, 2012, vol. 48, no. 1, pp. 75–84.

Kopytenko, E.A., Palshin, N.A., Poljakov, S.V., Schennikov, A.V., Reznikov, B.I., and Samsonov, B.V., New portable multifunctional broadband MT System, in *IAGA WG 1.2 on Electromagnetic Induction in the Earth. Abstracts of 20th Workshop, Giza, Egypt, September 18–24, 2010.*

Kuvshinov, A., Utada, H., Avdeev, D., and Koyama, T., 3D modeling and analysis of the DST EM responses in the North Pacific Ocean region, *Geophys. J. Int.*, 2005, no. 160, pp. 505–526.

Megerya, V.M., Filatov, V.G., Starostenko, V.I., Korchagin, I.N., Lobanov, A.M., Glasko, Yu.V., Volotskov, M.Yu., and Skachkov, S.A., Geosolitonic concept and prospects of application of non-seismic methods for prospecting hydrocarbons accumulations, in *Geophys. J.*, 2012, vol. 34, no. 3, pp. 4–21.

Parker, R.L., The inverse problem of electromagnetic induction: existence and construction of solutions based on incomplete data, *J. Geophys. Res.*, 1980, vol. 85, pp. 4421–4428.

Semenov, V.Yu., *Obrabotka dannykh magnitotellurichеskogo zondirovaniya* (Processing of Magnetotelluric Sounding Data), Moscow: Nedra, 1985.

Semenov, V.Yu. and Kharin, E.P., Electrical conductivity of the mantle from the data of Russian geomagnetic observatories, *Izv. Phys. Solid Earth*, 1997, vol. 33, no. 9, pp. 720–726.

Semenov V.Yu., Ádám A., Jówzˆiak W., Ladanyvskyy B., Logvinov I.M., Pek J., Pushkarev P., Vozar J., and Experimental Team of CEMES, Electrical structure of the upper mantle beneath Central Europe: Results of the CEMES project, *Acta Geophys.,* 2008, vol. 56, no. 4, pp. 957–981.

Shevtsov, A.N., Direct and inverse problems of frequency electromagnetic sounding with industrial power transmission lines, in *Teoriya i metodika glubinnykh elektromagnitnykh zondirovanii na kristallicheskikh shchitakh* (Theory and Methods of Deep Electromagnetic Sounding on Crystalline Shields), Apatity: KNTs RAN, 2006, pp. 171–181.

Tereshchenko, E.D., Grigoriev, V.F., Barannik, M.B., 2 Danilin, A.N., Efimov, B.V., Kolobov, V.V., Prokopchuk, P.I., Selivanov, V.N., Kopytenko, Yu.A., and Zhamaletdinov, A.A., A Set–Up Converter and Energy Transfer System of the "Energy-2" Generator for Electromagnetic Sounding and Monitoring of Zones of Earthquake Sources, *Seism. Instrum.*, 2009, vol. 45, no. 1, pp. 119–133.

Tereshchenko, E.D., Grigoryev, V.F., Barannik, M.B., 2 Danilin, A.N., Efimov, B.V., Kolobov, V.V., Prokopchuk, P.I., Selivanov, V.N., Kopytenko, Yu.A., and Zhamaletdinov, A.A., A Set-up converter and energy transfer system of an "Energy-2" generator for electromagnetic sounding and monitoring of zones of earthquake sources, *Seism. Instrum.*, 2009, vol. 45, no. 2, pp. 119–137.

Vanyan, L.L., *Osnovy elektromagnitnykh zondirovanii* (Basics of Electromagnetic Soundings), Moscow: Nedra, 1965.

Velikhov, E.P., Zhamaletdinov, A.A., Sobchakov, L.A., Veshev, A.V., Saraev, A.K., Tokarev, A.D., Shevtsov, A.N., Vasil'ev, A.V., Sonnikov, A.G., and Yakovlev, A.V., Experience of frequency electromagnetic sounding of the Earth's crust using a high-power ULF antenna, *Dokl. Ross. Akad. Nauk*, 1994, vol. 338, no. 1, pp. 106–109.

Vozar, J. and Semenov, V.Y., Compatibility of induction methods for mantle soundings, *J. Geophys. Res.*, 2010, vol. 15, B03101. doi: 10.1029/2009JB006390

Zhamaletdinov, A.A., Efimov, B.V., and Shevtsov, A.N., Soundings with high-power controlled sources in combination with MT soundings (CSMT): Prospects for oil and gas prospecting, in *Innovatsionnye elektromagnitnye metody geofiziki* (Innovative Electromagnetic Methods in Geophysics), Velikhov, E.P, Ed., Moscow: Nauchnyi Mir, 2009, pp. 95–113.

Zhamaletdinov, A.A., *Teoriya i metodika glubinnykh elektromagnitnykh zondirovanii s moshchnymi kontroliruemymi istochnikami (opyt kriticheskogo analiza)* (Theory and Techniques if Deep Electromagnetic Sounding with High-Powser Controlled Sources: Critical Review Essay), St. Petersburg: SOLO, 2012.

Translated by M. Nazarenko

SPELL: 1. Фаза7, 2. Barannik